

Compositional Dependence on Structural and Electrical Properties of $Mg_x Zn_{1-x}O$ Thin Films Prepared by Sol-Gel Method

P.Sateesh¹, P. Madhusudana Rao²

Research Scholar, Department of Physics, JNTU Hyderabad, Telangana, India¹

Professor of Physics, Department of Physics, JNTUH College of Engineering, Hyderabad, Telangana, India²

ABSTRACT: $Mg_xZn_{1-x}O$ thin films with various content ratio ranging from 0.07 to 0.57 were prepared by sol-gel spin coating method. To investigate the effects of content ratio on the structural and the optical properties of the $Mg_xZn_{1-x}O$ thin films, Scanning Electron Microscopy (SEM) and X-ray diffraction (XRD) are carried out. Electrical properties of thin films are also investigated. With increase in the content ratio, the grain size of the $Mg_xZn_{1-x}O$ thin film was found to be increased. The energy dispersive analysis by X-ray (EDAX) confirmed the element of Mg in the ZnO films. Growth of high quality MgZnO nanostructured thin films opens up numerous possibilities for the development of ultraviolet optoelectronic devices.

KEYWORDS: Mg doped ZnO, Nanostructured thin film, spin coating, Microstructure

I. INTRODUCTION

Semiconductor nanoparticles show unique, size-dependent optical properties due to quantum confinement effect. Zinc Oxide (ZnO) is a wide-band gap II-IV semiconductor material with 3.2 eV optical band gap and having large exciton binding energy of ~60 meV which causes the stimulated emission at room temperature. Hall mobility ZnO single crystal is on the order of $200 \text{ cm}^2 \text{ v}^{-1} \text{ s}^{-1}$ at room temperature. An emerging material that holds promise for flexible applications is ZnO. Due to its deep excitonic energy level, thermal stability, and chemically benign nature [1-4], ZnO is increasingly become an attractive wide band gap semiconductor [5]. Most of the group II-VI binary compound semiconductors crystallize in either cubic zinc blende or hexagonal wurtzite structure where each anion is surrounded by four cations at the corners of a tetrahedron, and vice versa. This tetrahedral coordination is typical of sp^3 hybridized covalent bonding. It has a polar hexagonal axis, the c axis, chosen to be parallel to z. This is a hexagonal lattice, with lattice parameters $a = b = 0.3296$ and $c = 0.52065$ nm, and is characterized by two interconnecting hexagonal sub lattices of Zn^{2+} and O^{2-} , such that each Zn ion is surrounded by tetrahedral of O ions and vice versa. This tetrahedral coordination gives rise to polar symmetry along the hexagonal axis.

II. MATERIALS AND METHODS

Zinc oxide (ZnO) and its alloys are semiconductors which offer potential applications such as solar cells, display panel electrodes, light emitters, sensors, modulators and acoustic surface wave devices [6,7]. Mg is incorporated as substitution type material to control the bandgap in ternary oxide semiconductors [8, 9]. Although Mg^{2+} (0.57 Å) has a similar ionic radius to Zn^{2+} (0.60 Å), the solid solubility of MgO in the ZnO matrix is limited due to its different crystal structure. MgO has a cubic rock salt structure, [10] while ZnO has a hexagonal wurtzite structure [11]. So, the reports have demonstrated that the MgZnO alloy thin films with a wide range of Mg^{2+} from 0 to 36% still maintained the hexagonal lattice structure due to the similar ionic radius of Mg^{2+} and Zn^{2+} , and corresponding energy bandgap could be increased from 3.34 to 3.96 eV [12]. MgZnO films can be prepared by several techniques such as molecular beam epitaxy (MBE) [10], metal-organic chemical deposition (MOCVD) [11], RF magnetron co-sputtering [12], pulse laser

International Journal of Innovative Research in Science, Engineering and Technology

(An ISO 3297: 2007 Certified Organization)

Vol. 4, Issue 6, June 2015

deposition (PLD) [13] and sol-gel[14]. The sol-gel method has several advantages such as simple and low cost. The most wide spread use of sol-gel is in coating of devices such as in antireflective coatings with Index gradation; optical or infrared absorbing coatings and electrically conductive coatings. Until now, very little work has been done in MgZnO thin films by using sol-gel method. In this study, sol-gel spin-coating method was adopted to deposit the $Mg_xZn_{1-x}O$ thin films with various Mg mole fractions because spin-coating technique has distinct advantages such as easy and cheap operation, excellent compositional control and homogeneity on the molecular level.

III. EXPERIMENTAL DETAILS

The $Mg_xZn_{1-x}O$ thin films were grown on Si (100) sub-strates by using sol-gel spin-coating method. The Si substrates were cleaned by immersion in an acetone for 24 hours and then also cleaned with 55 deg⁰C of 10% NaOH solution and then rinsed with deionized water. The preparation of $Mg_xZn_{1-x}O$ thin films is illustrated schematically in Figure 1. The precursor sol solution was prepared by dissolving 0.6 M zinc acetate dihydrate [$Zn(CH_3COO)_2 \cdot 2H_2O$] in 0.6 M 2-methoxyethanol as a solvent, and monoethanol-amine (MEA) was added to the stable solution. The molar ratio of zinc acetate dihydrate to 2-methoxyethanol was maintained at 1:1. The Mg mole fraction was controlled by the change in the wt % ratio of magnesium acetate tetrahydrate [$Mg(CH_3COO)_2 \cdot 4H_2O$] to zinc acetate dihydrate from 0.07 to 0.57. The resultant sol solution was stirred at 60 °C for 2 h to yield a clear and homogenous solution. The sol solution was preserved for 1 day before the growth of the $Mg_xZn_{1-x}O$ thin films. The sol solution was spin-coated onto Si substrate, rotated at 3000 rpm for 20s. The $Mg_xZn_{1-x}O$ thin films were heated at 300 °C for 10 min to evaporate the solvent and remove the organic residuals (named as pre-heat treatment). After the pre-heat treatment, the $Mg_xZn_{1-x}O$ thin films were cooled with a cooling rate of 5°C/min to avoid cracks. The spin-coating and pre-heating processes were repeated three times. In order to crystallize, the $Mg_xZn_{1-x}O$ thin films were heated in a furnace under an air atmosphere at 500 °C for 1 h (named as post-heat treatment). The effects of Mg mole fraction on the structural and the optical properties of the $Mg_xZn_{1-x}O$ thin films were investigated by Scanning Electron Microscopy (SEM), X-ray diffraction (XRD), and Fourier transform infrared spectroscopy (FT – IR).

Table1: The sample notation and the doping rate of $Mg_x Zn_{1-x}O$ samples

Sample name	Doping rate 1-x	(Mol %) X
P1	99.93	0.07
P2	99.83	0.17
P3	99.73	0.27
P4	99.63	0.37
P5	99.53	0.47
P6	99.43	0.57

International Journal of Innovative Research in Science, Engineering and Technology

(An ISO 3297: 2007 Certified Organization)

Vol. 4, Issue 6, June 2015

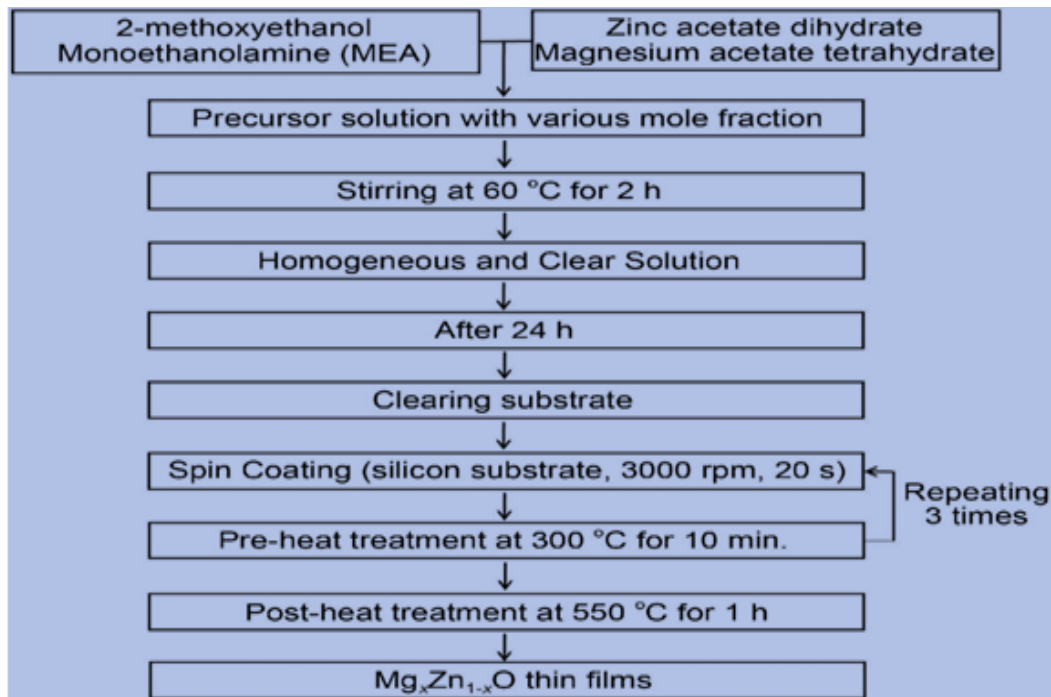
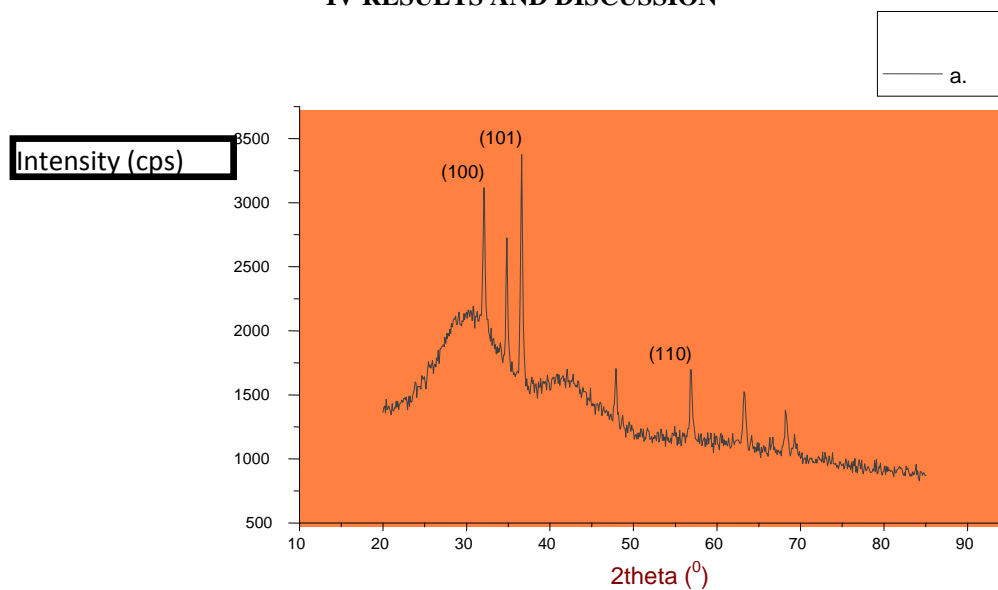


Figure1: Flow chart for the preparation of the $Mg_xZn_{1-x}O$ thin films by sol-gel spin-coating method.

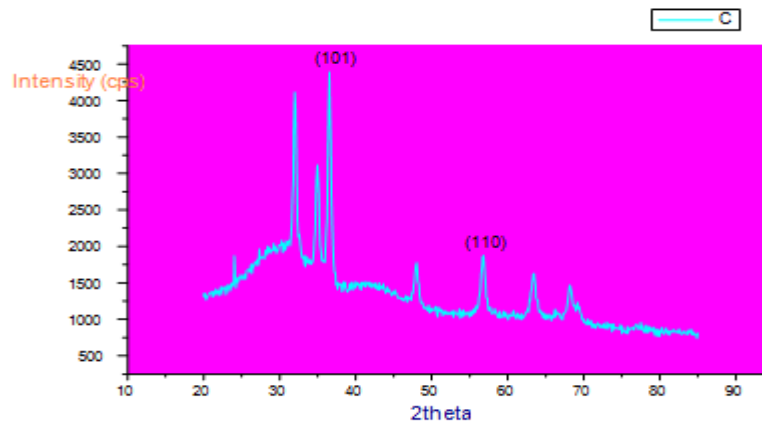
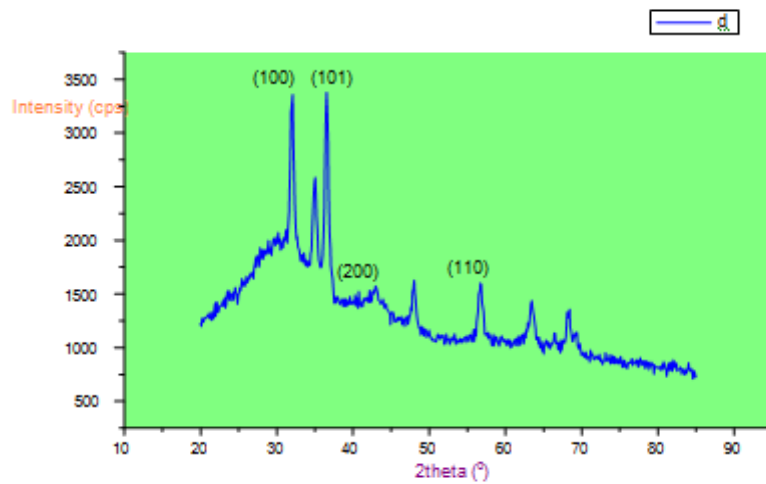
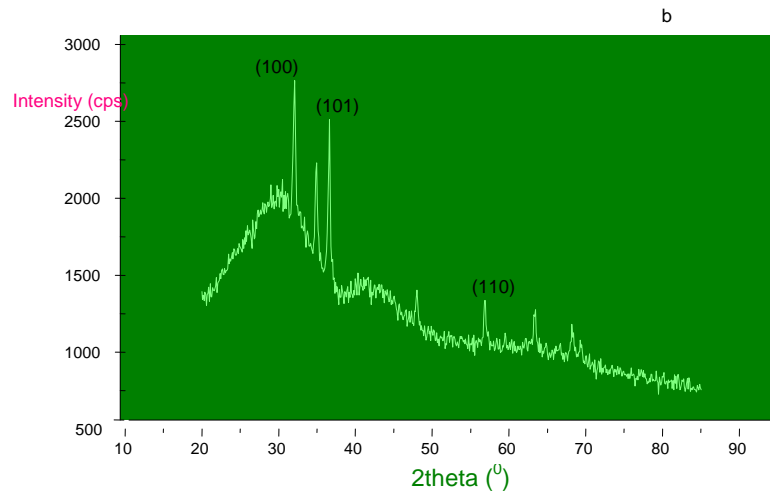
IV RESULTS AND DISCUSSION



International Journal of Innovative Research in Science, Engineering and Technology

(An ISO 3297: 2007 Certified Organization)

Vol. 4, Issue 6, June 2015



International Journal of Innovative Research in Science, Engineering and Technology

(An ISO 3297: 2007 Certified Organization)

Vol. 4, Issue 6, June 2015

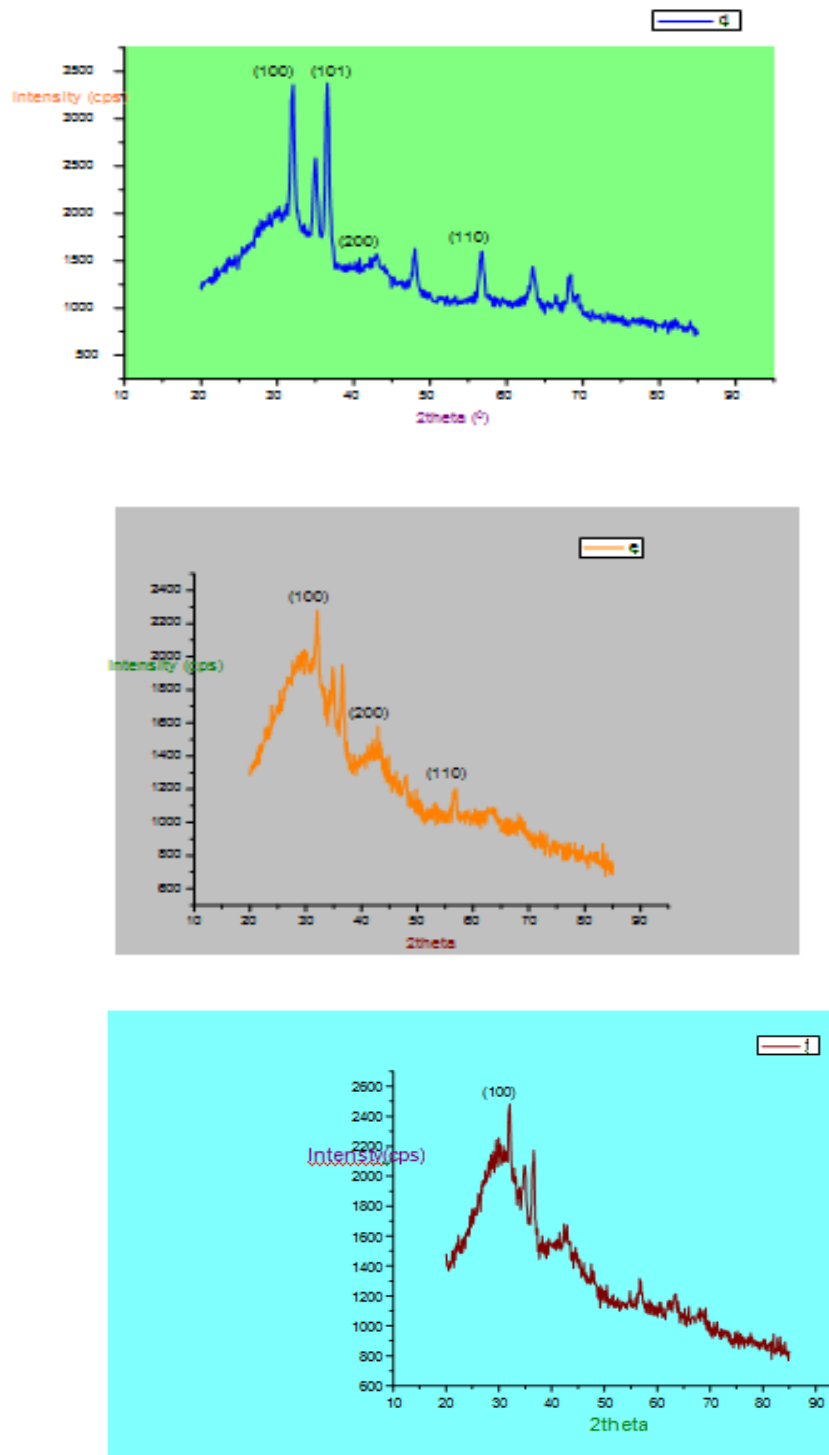


Figure 2: XRD pattern of the $Mg_xZn_{1-x}O$ thin films with various content ratio of magnesium acetate tetrahydrate to zinc acetate dihydrate; (a) 0.07 (b) 0.17, (c) 0.27, (d) 0.37, (e) 0.47, and (f) 0.57.

International Journal of Innovative Research in Science, Engineering and Technology

(An ISO 3297: 2007 Certified Organization)

Vol. 4, Issue 6, June 2015

The XRD patterns of the $Mg_xZn_{1-x}O$ thin films with different content ratio of magnesium acetate tetra-hydrate to zinc acetate dihydrate. From all the $Mg_xZn_{1-x}O$ thin films, four ZnO diffraction peaks at 31° , 34° , 36° and 56° are observed, corresponding to ZnO (100), (002), (101), and (110), respectively. The intensity of the diffraction peak at 34° from the MgZnO thin films ($0.05 \leq x \leq 0.4$) is stronger than that of the ZnO, which indicates that preferred growth direction is along the c-axis with [001] crystal orientation. It is well-known that ZnO is usually grown with c-axis preferred orientation under typical growth conditions because of the lowest surface energy of the (001) basal plane in ZnO, leading to a preferred growth in the [001] direction.²² In general, the intensity of the (002) diffraction peak of $Mg_xZn_{1-x}O$ films was decreased with increase in the Mg content due to the degraded crystallographic characteristics²³. It was assumed that the enhancement in the (002) diffraction peak was due to increase in the oxygen affinity between Zn and O caused by the incorporation of MgO. The dynamic affinity of the Zn for bonding with O might be improved by the incorporation with a suitable amount of MgO due to the oxygen affinity of the Mg is larger than that of the Zn. The relatively stronger bond between Mg and O leads to the existence of more oxygen, in sequence; the more stoichiometric ZnO crystals were generated in the $Mg_xZn_{1-x}O$ thin films. As a result, the intensity of the (002) diffraction peak from the $Mg_xZn_{1-x}O$ thin films with the Mg content ratio of 0.05 was much stronger than that of the ZnO. However, the intensity of the (002) diffraction peak was again decreased further increase in the content ratio, which was because the influence of the degraded crystallographic characteristics became larger than that of the stoichiometric improvement. To demonstrate that further studies will be needed. The formation of MgO on surface of the MgZnO thin films was observed as evidenced by the appearance of MgO (200) diffraction peak at 43° , indicating that the Mg content exceeded its solubility limit in the MgZnO alloys. Figure 2; (a) 0.07 (b) 0.17, (c) 0.27, (d) 0.37, (e) 0.47, and (f) 0.57 Presents XRD spectra of ZnO nanoparticles doped with various Mg doping concentrations. There are seven broad peaks corresponding to (1 0 0), (2 0 0), (1 0 1), (1 0 2), (1 1 0), (1 0 3) and (1 1 2) which have been indexed to the standard pattern of hexagonal ZnO.

Table2: Structural parameters of $Mg_xZn_{1-x}O$ thin films

sample	2 θ (Degree)	h k l	FWHM (degree)	d- spacing (\AA)	D (nm)
$Mg_{0.07}Zn_{0.93}O$	36.61	111	0.36	2.4540	23.253
$Mg_{0.27}Zn_{0.73}O$	36.54	101	0.54	2.4580	15.499
$Mg_{0.37}Zn_{0.63}O$	36.55	101	0.67	2.4582	12.492

Table2: Presents the average particle size of MgZnO samples was estimated with the width of the lines in the XRD spectrum using the Scherrer equation that is given below

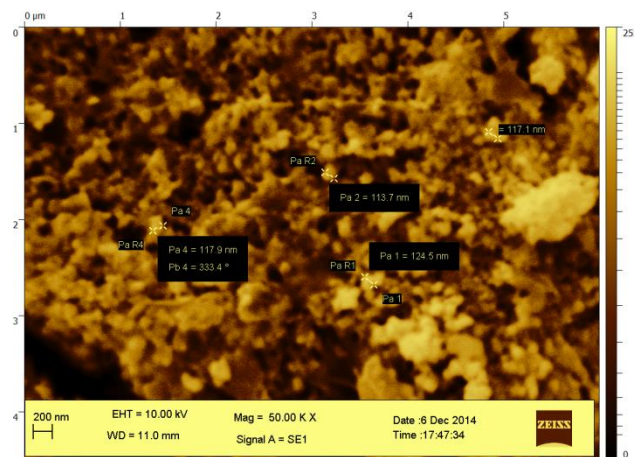
International Journal of Innovative Research in Science, Engineering and Technology

(An ISO 3297: 2007 Certified Organization)

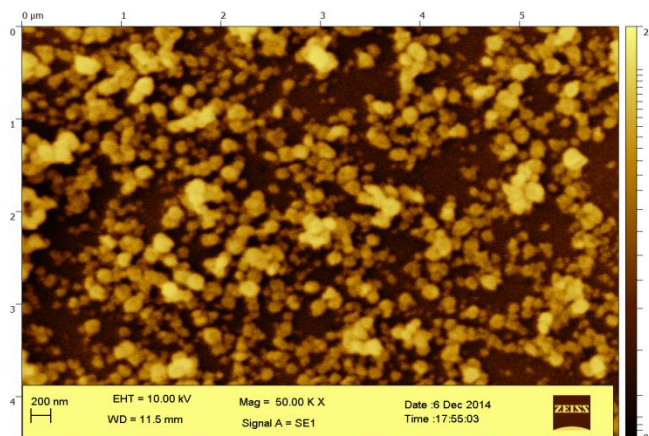
Vol. 4, Issue 6, June 2015

$$d = K\lambda / \beta \cos \theta$$

Where k is the unit less constant taken as 0.9, λ is the X-ray wave length (1.5406 Å), β is the width of the line at the half maximum intensity and θ is the half of the diffraction angle. The estimated particle sizes of samples with different mg concentrations are given in **Table1**. The particle size is gradually decreased with increase of Mg doping. As the Mg concentration increases, the optical band gap also increases because of the replacement of Mg with Zn in the crystal lattice (MgO has a higher band gap (7.8 eV) than that of ZnO (3.4 eV)). Also, the XRD patterns of Mg-doped ZnO samples show a slight shifting of the centre of diffraction peaks toward higher angle compared to pure ZnO [15].



0.07(a)

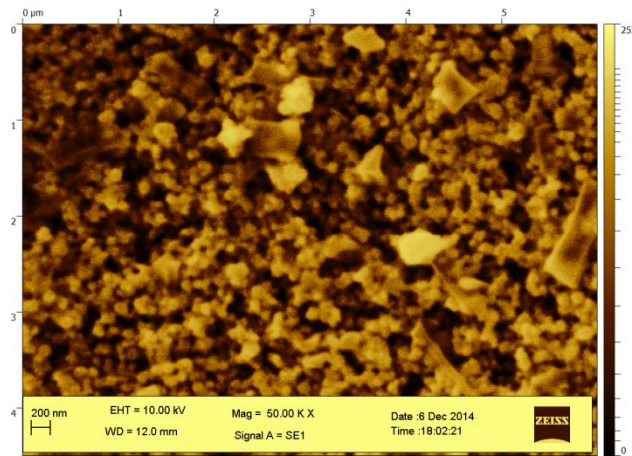


0.17(b)

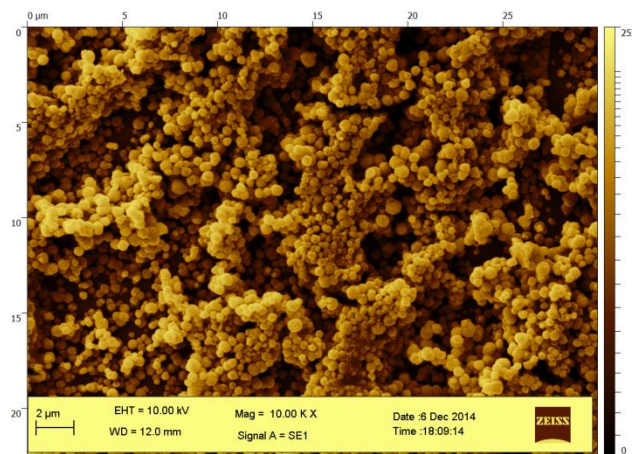
International Journal of Innovative Research in Science, Engineering and Technology

(An ISO 3297: 2007 Certified Organization)

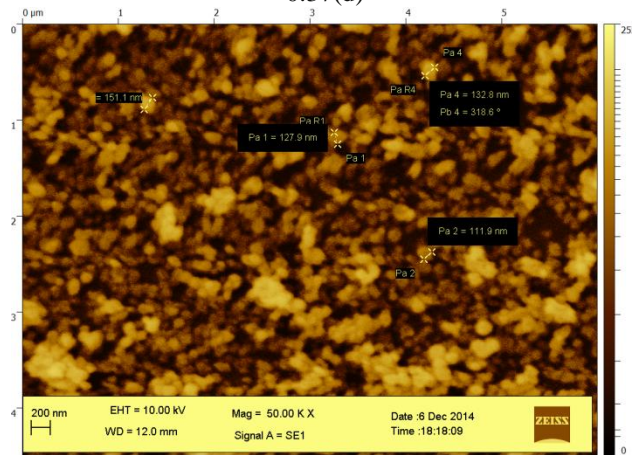
Vol. 4, Issue 6, June 2015



0.27(c)



0.37(d)

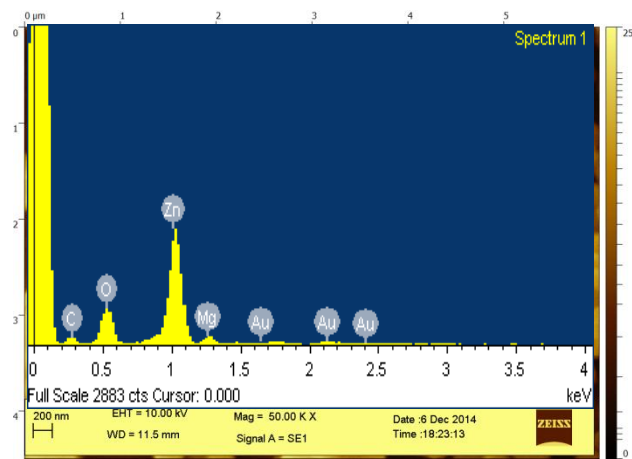


0.47(e)

International Journal of Innovative Research in Science, Engineering and Technology

(An ISO 3297: 2007 Certified Organization)

Vol. 4, Issue 6, June 2015

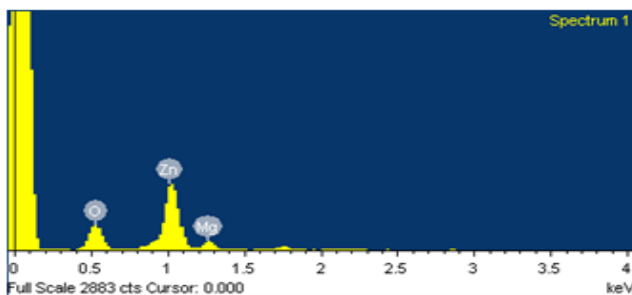


0.57(f)

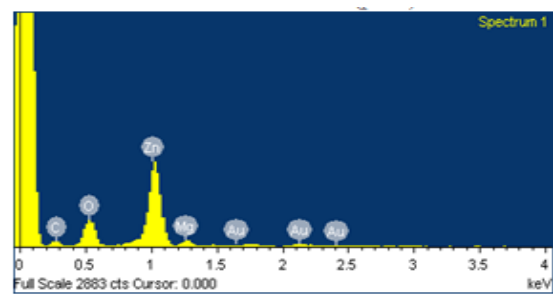
Figure 3: SEM images of the $Mg_xZn_{1-x}O$ thin films with various content ratio of magnesium acetate tetrahydrate to zinc acetate dihydrate; (a) 0.07 (b) 0.17, (c) 0.27, (d) 0.37, (e) 0.47, and (f) 0.57

SEM images of the $Mg_xZn_{1-x}O$ thin films with different content ratio of magnesium acetate tetra-hydrate to zinc acetate dihydrate; (a)0.07(b) 0.17, (c) 0.27, (d) 0.37, (e) 0.47, and (f) 0.57All the $Mg_xZn_{1-x}O$ thin films exhibit a rough surface with the three-dimensional (3D) island growth.

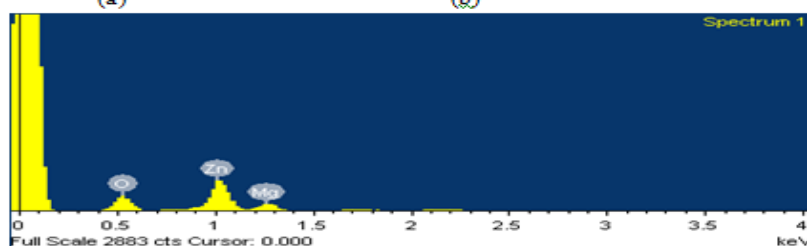
The number of the voids was decreased with increase in the content ratio of the $Mg_xZn_{1-x}O$ thin films. The incorporation of Mg in $MgZnO$ thin films may promote lateral growth and favor layer-by-layer growth with smooth surface in comparison to the ZnO thin films on Si as the increase in the Mg content. The particle size for the pressed $Mg_{0.07}Zn_{0.93}O$ and $Mg_{0.37}Zn_{0.63}O$ are in the range of 120 to 200nm. It may be agglomeration of $ZnMgO$ particles due to pressing the particles and triethanolamine which was used to improve adhesion of solution.



(a)



(b)



(c)

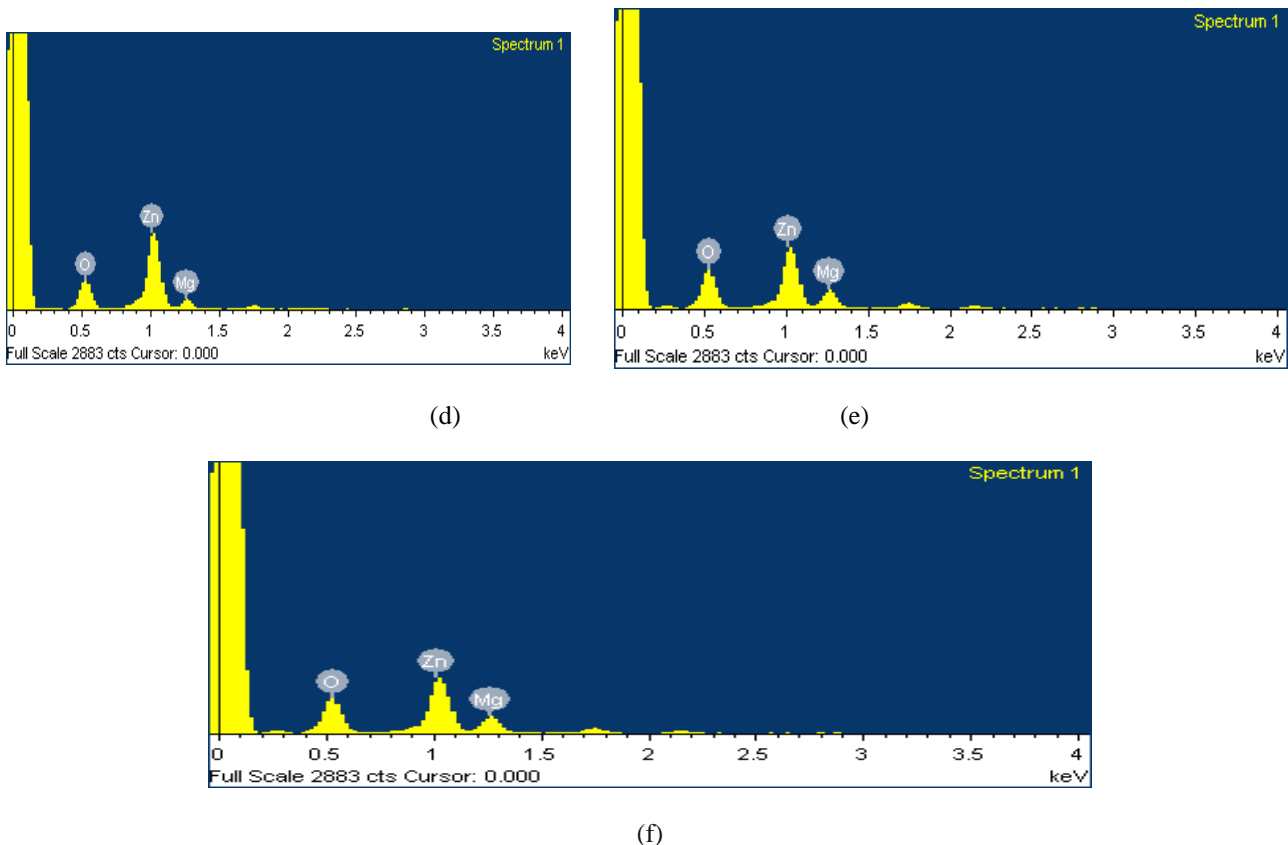


Figure 4: EDX spectra of ZnO nanoparticles doped with (a) 0.07, (b) 0.17 (c) 0.27 and (d) 0.37(e) 0.47(f) 0.57 Mg concentrations. Samples were annealed at 550°C

The EDS spectrum analysis shows Mg Zn peaks. The Mg incorporation and percentage of Mg in doped ZnO samples were analyzed by energy-dispersive X-ray (EDX) spectroscopy (figure 4). It is observed that in most of the cases the EDX may have estimated the actual Mg in the samples. EDX spectrum of $Mg_xZn_{1-x}O$ thin films after annealing at 550 °C for 30 min is seen in figure 4. Zn and Mg peaks are clearly seen.

V CONCLUSIONS

The structural and optical properties of the $Mg_xZn_{1-x}O$ thin films with the various content ratio grown by sol-gel spin-coating method were investigated. The $Mg_xZn_{1-x}O$ thin films exhibit island growth and the grain size was increased with content ratio. $MgZnO$ thin films are highly transparent with sharp absorption edges. Typical film thicknesses were found to increase from 120 nm to 200nm for annealed at 550°C.

VI ACKNOWLEDGMENTS

The basic research was supported by JNTUH. The SEM, XRD and EDX analysis of samples is facilitated by OU and HCU Universities.

International Journal of Innovative Research in Science, Engineering and Technology

(An ISO 3297: 2007 Certified Organization)

Vol. 4, Issue 6, June 2015

REFERENCES

- [1] B. B. Rao, Mater Chem. Phys. 64, 62 (2000).
- [2] R. W. Birkmire and E. Eser, Annu. Rev. Mater Sci. 27, 625 (1997).
- [3] T. Aoki, Y. Hatanaka, and D. C. Look, Appl. Phys. Lett. 76, 3257 (2000).
- [4] S. J. Pearton, D. P. Norton, K. Ip, Y. W. Heo, and T. Steiner, Prog. Mater. Sci. 50,293 (2005).
[5] G. H. Ning, X. P. Zhao, and J. Li, Opt. Mater. 27, 1 (2004).
- [6] Z. Q. Ma, W. G. Zhao, and Y. Wang, Thin Solid Films 515, 8611 (2007).
- [7] L. Zhuang and K. H. Wong, Thin Solid Films 516, 5607 (2008).
- [8] E. Barsoukov and J. R. Macdonald, Impedance Spectroscopy: Theory, Experiment, and Applications, Second Edition (Wiley InterScience, New Jersey, 2005).
- [9] Z. K. Haiba and L. Arda, Cryst. Res. Technol. 44, 845 (2009).
- [10] P. Bhattacharya, R. R. Das, and Ram S. Katiyar, Thin Solid Films 447-448, 564 (2004).
- [11] S. J. Pearton, D. P. Norton, K. Ip, Y. W. Heo, and T. Steiner, Prog. Mater. Sci. 50, 293 (2005).
- [12] S. J. Pearton, D. P. Norton, K. Ip, Y. W. Heo, and T. Steiner, J. Vacuum Sci. Technol. B 22, 932 (2004).
- [13] T. Ghosh, M. Dutta, S. Mridha, and D. Basak, J. Electrochem. Soc. 156, H285 (2009).
- [14] J. P. Han, P. Q. Mantas, and A. M. R. Senos, J. Eur. Ceram. Soc. 22, 49 (2002).
- [15] J. P. Han, P. Q. Mantas, and A. M. R. Senos, J. Eur. Ceram. Soc. 21, 1183 (2001).